Volume 2
Number 1
1 January 2025
Pages 1–294

RSC Applied Interfaces

rsc.li/RSCApplInter

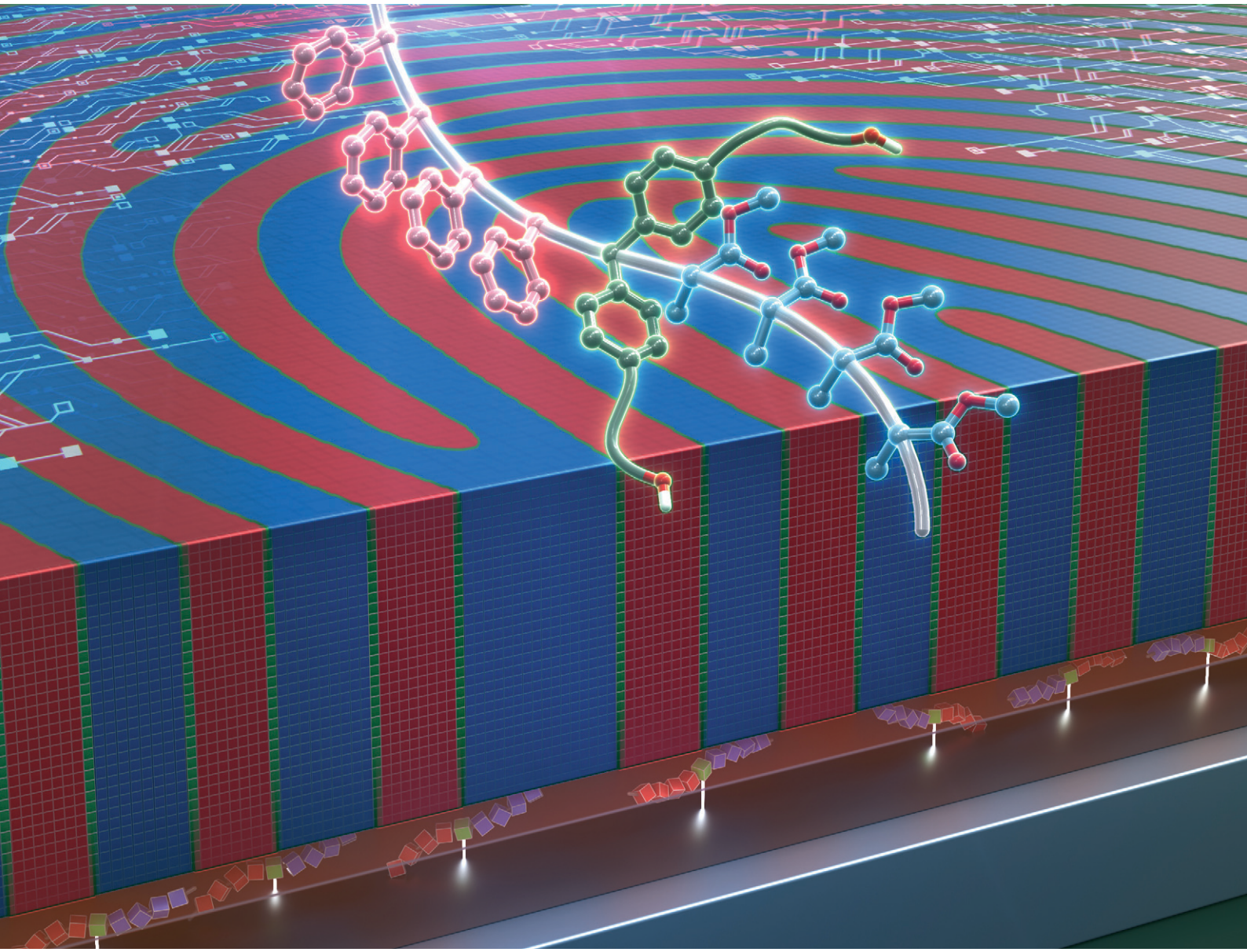

ISSN 2755-3701

ROYAL SOCIETY OF CHEMISTRY

PAPER

Teruaki Hayakawa *et al.*

Dual function of precisely modified hydroxy-PS-*b*-PMMA as neutral layers and thin films for perpendicularly oriented lamella

RSC Applied Interfaces

ROYAL SOCIETY OF CHEMISTRY

PAPER

View Article Online
View Journal | View Issue

Cite this: *RSC Appl. Interfaces*, 2025, **2**, 74

Dual function of precisely modified hydroxy-PS-*b*-PMMA as neutral layers and thin films for perpendicularly oriented lamella†

Riku Mizusaki,[a] Shinsuke Maekawa,[a] Takehiro Seshimo,[b] Takahiro Dazai,[b] Kazufumi Sato,[b] Kan Hatakeyama-Sato,[a] Yuta Nabae[a] and Teruaki Hayakawa *[a]

Received 3rd June 2024,
Accepted 19th August 2024

DOI: 10.1039/d4lf00197d

rsc.li/RSCApplInter

We propose a facile and fast control method to obtain perpendicularly oriented microphase-separated structures in block copolymer (BCP) thin films for nanopatterning with a BCP lithography technique. By synthesizing a derivative of polystyrene-*block*-poly(methyl methacrylate) (PS-*b*-PMMA) with precisely introduced two hydroxy groups at the junction (PS-$(OH)_2$-PMMA) and by applying it onto silicon substrates, we investigated the lamellar orientations in PS-$(OH)_2$-PMMA thin films with respect to the annealing time of neutral layers (NLs) for modifying silicon substrates to neutralize the interfacial free energies between the substrate and each block component in the BCP thin films. Various NLs, including PS-$(OH)_2$-PMMA itself, were applied onto silicon substrates, and PS-$(OH)_2$-PMMA has turned out to take a dual role of BCP thin films for nanopatterning and NLs, which shows its supremacy over other methods. PS-$(OH)_2$-PMMA needs only 20 minutes of annealing to form NLs that sufficiently neutralize the substrates and induce perpendicular lamellae, which is a significant improvement over non-functionalized PS-*b*-PMMA. This result highlights the enhanced adsorbability of BCP neutral layers by the introduction of only a small amount of hydroxy groups.

Introduction

Block copolymers (BCPs) exhibit diverse microphase-separated structures by self-assembly depending on the volume fraction of each block component, the degree of polymerization (N), and the Flory–Huggins interaction parameter (χ).[1,2] Among these structures, periodically aligned structures such as lamellae, or hexagonally packed cylinders are widely studied as candidates for nanopatterns for one of the next generation silicon wafer fabrication techniques, which is called BCP lithography.[3,4] In BCP lithography, the microphase-separated structure in the thin films for nanopatterning is aligned *via* the directed self-assembly (DSA) method and thus should be oriented perpendicularly to the substrates to obtain a fine and high-resolution pattern.[5–10]

Typically, the orientation of microphase-separated structures in a BCP thin film on a substrate is determined by the balance between the different interfacial free energies of the polymer/substrate interface and the polymer/air interface for each block component. Thus, one component is likely to form domains at the BCP/substrate interface and another component is likely to form domains at the surface.[11] As a result, the overall microphase-separated structure has a parallel orientation, which is not applicable to BCP lithography practically. Therefore, one of the general and indispensable methods is to use a neutral layer (NL), which is an interface modifying material to neutralize the BCP/substrate interface, to obtain a perpendicularly oriented microphase-separated structure.[12,13] As for polystyrene-*block*-poly(methyl methacrylate) (PS-*b*-PMMA), which is a representative material of lithographic templates due to its wide process window[14,15] and selectivity in etching process,[16–21] the microphase-separated structures can be oriented perpendicularly only by neutralizing the BCP/substrate interface because PS and PMMA is believed to have almost the same value of surface free energy at the annealing temperature for microphase-separation.[22]

The basic materials for NLs are random copolymers (RCPs), which consist of the same components as those of BCPs for thin films and additional hydroxy-group-containing units, often referred to as RCP brush or mat.[12–15] This is attributed to the belief that introducing hydroxy groups into the polymers for NLs contributes to better adsorbability of NLs to silicon substrates *via* physical interactions such as hydrogen bonds, van der Waals forces, and dipolar interactions or chemical

[a] *School of Materials and Chemical Technology, Tokyo Institute of Technology, 2-12-1-S8-36 Ookayama, Meguro-ku, Tokyo, Japan.*
E-mail: hayakawa.t.ac@m.titech.ac.jp
[b] *TOKYO OHKA KOGYO CO., LTD., 1590 Tabata, Samukawa-machi, Koza-gun, Kanagawa, Japan*

† Electronic supplementary information (ESI) available. See DOI: https://doi.org/10.1039/d4lf00197d

reactions with silanol groups in the native oxide layer of silicon substrates.[12,23] Such chemical reaction or physical interaction would help the polymers to be grafted or to be adsorbed to the silicon substrates, ensuring the sufficient formation of NLs. However, in RCPs, the number and the positions of hydroxy groups are not precisely controlled. Thus, the effect on the improvement of adsorbability to silicon substrates by the introduction of a hydroxy group is difficult to be evaluated, and the optimal number of hydroxy groups in NLs has still not been studied in detail.[12–15] In addition, the hydroxy groups that are not involved in adsorption possibly cohere and make domains, which would be one of the causes of structural defect generation in DSA patterns.[24] Therefore, it is expected to provide further insights into the effects of hydroxy groups by controlling the number or the positions of hydroxy groups introduced in a molecule composing NLs.

In addition, BCP lithography conventionally requires the use of two different polymers, RCPs for NLs and BCPs for thin films, and to achieve perpendicular orientation of the microphase-separated structure in thin films, it is necessary to optimize the monomer composition in NLs.[12–15] Consequently, the use of BCPs as NLs was studied in previous studies.[25–27] In one of the previous studies,[25] a physisorption layer of PS-*b*-PMMA was used as NLs and perpendicularly oriented lamellae were obtained in thin films of PS-*b*-PMMA, indicating the applicability of BCPs as NLs, and dual-use potential of the same polymer for both NLs and thin films. However, it took 24 h annealing time for NLs to promote physisorption of BCP molecules to substrates, which is much longer than the annealing time of several minutes for the adsorption of RCP neutral layers. Therefore, the use of BCPs that have hydroxy groups is effective in improving the BCP neutral layers in terms of shortening the annealing time for NL adsorption.

In this study, we designed and synthesized lamella-forming PS-$(OH)_2$-PMMA with two hydroxy groups at the junction point of PS and PMMA according to Scheme 1. Using this polymer as both NLs and thin films, we assessed how hydroxy groups in NLs affected adsorbability to silicon substrates. For the control experiment, non-functionalized PS-*b*-PMMA and poly[styrene-*ran*-(methyl methacrylate)-*ran*-(2-hydroxyethyl methacrylate)] (P(S-*r*-MMA-*r*-HEMA)), which is one of the typical materials for NLs, were also synthesized and applied as NLs. The rapidity of perpendicular lamella formation in PS-$(OH)_2$-PMMA thin films, depending on the variety of NLs, was observed by atomic force microscopy (AFM) to evaluate the ability of PS-$(OH)_2$-PMMA as an NL material. Our results show that the introduction of two hydroxy groups at the junction of PS and PMMA enhanced the adsorbability of the BCP to the substrate, thereby reducing the annealing time of NLs.

Experimental

Materials

The reagents were purchased and used as received unless otherwise noted. Styrene and methyl methacrylate (MMA) were distilled under reduced pressure in the presence of calcium hydride and used in free radical polymerization, and for living anionic polymerization, they were degassed in the presence of *n*-butyl-*sec*-butylmagnesium or trioctylaluminum respectively by the freeze–pump–thaw method and purified by trap-to-trap distillation. 1,1-Diphenylethylene (DPE) was degassed in the presence of *n*-butyllithium by the freeze–pump–thaw method and purified by trap-to-trap distillation. 2-Hydroxyethyl methacrylate (HEMA) was dehydrated by activated alumina.

Substrates

Standard silicon wafers with the native oxide layer (~2 nm) were cut into pieces (~1.5 cm square) and treated as the following. A silicon substrate was wiped with lens-cleaning paper soaked with toluene and then successively sonicated by acetone, ethanol, and toluene in this order for 1 minute each. The substrate was blown with N_2 and heated on a hotplate at 100 °C for 1 minute to remove the residual solvents, and then used in the following experiments.

Measurements

Both ^1H and ^{13}C NMR (nuclear magnetic resonance) spectroscopy were conducted on a JEOL JNM-ECS400. FT-IR

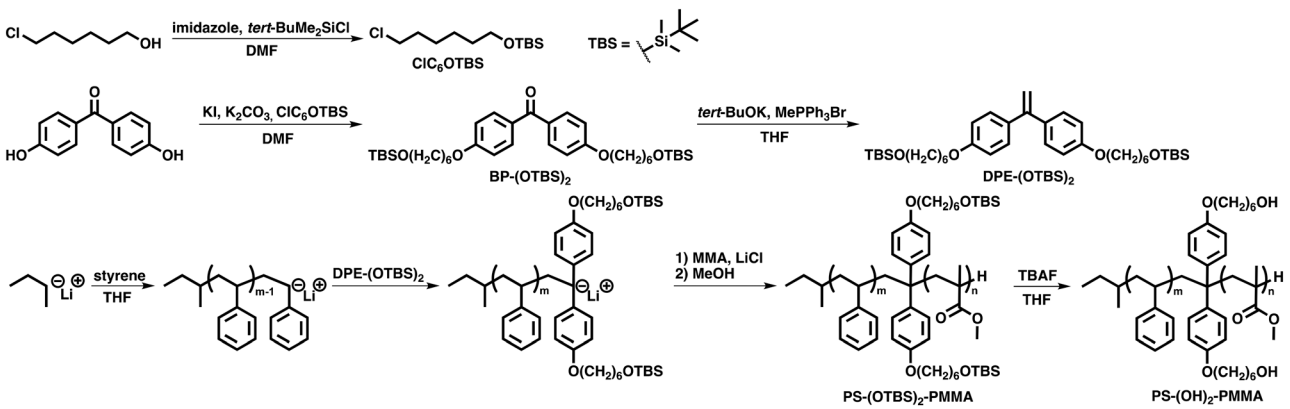

Scheme 1 The synthetic route of PS-$(OH)_2$-PMMA.

(Fourier-transform infrared) spectroscopy was conducted on a JASCO FT/IR-4100 using a KBr pellet or KBr plate for solid samples or liquid samples respectively. SEC (size exclusion chromatography) was conducted on an apparatus consisting of a SHIMADZU Prominence501 and a RESONAC RI501, using THF as eluent and Shodex GPC LF-804 as columns. The calibration curve was prepared by standard PS. Measurements were conducted at a flow rate of 1 mL min^{-1} and 40 °C. SAXS (small angle X-ray scattering) was conducted on an apparatus consisting of a Bruker NANOSTAR and a VÅNTEC-500. CuKα radiation (λ = 1.5416 Å) was generated under the conditions of 50 kV and 50 mA. The samples were prepared by slowly evaporating the solvent from 10 wt% THF solutions of each polymer at 25 °C in air and dried at room temperature in vacuum. The obtained films were then annealed at 180 °C for 24 h in vacuum and used for SAXS. TG (thermogravimetry) was conducted on a Hitachi High-Tech TG/DTA 7300 at a heating rate of 10 °C min^{-1} in the range from 30 °C to 550 °C. AFM was conducted on a JPK Instruments Nano Wizard Ultra Speed A in AC mode using Tap-300 as cantilevers. For the observations, a polymer thin film was spin-coated on a silicon substrate, which was treated as above, from 1 wt% PGMEA (propylene glycol 1-monomethyl ether 2-acetate) solution of the polymer, and then annealed at 250 °C under N_2 to facilitate the formation of a neutral layer. Next, unattached polymer chains were rinsed with PGMEA to obtain a neutral layer. Subsequently, the PS-$(OH)_2$-PMMA thin film (~30 nm) was spin-coated onto the neutral layer and annealed at 230 °C for 10 minutes under N_2 to facilitate microphase-separation after one-minute pre-baking at 90 °C under air. Film thicknesses were determined by interferometric spectroscopy using a Filmetrics F20. FE-SEM (field emission scanning electron microscopy) was conducted on a Hitachi High-Tech SU9000. Samples were prepared from the samples for AFM observation. For the cross-sectional view, aqueous solution of RuO_4 (0.5%) was dropped on the substrates and they were left still for 90 minutes. For the tilted view, the substrates with the PS-$(OH)_2$-PMMA thin film were put in a vacuum electron stainer (Filgen VSC1R1H) and stained with RuO_4 under the conditions of 500 Pa and 30 minutes. Then, the substrates were cut in liquid N_2 and observed by FE-SEM. FE-SEM observation was conducted at the acceleration voltage of 3.0 kV.

Synthesis of 1-(*tert*-butyldimethylsiloxy)-6-chlorohexane (ClC_6OTBS)

Imidazole (2.71 g, 39.8 mmol) and 6-chloro-1-hexanol (2.73 g, 20.0 mmol) were dissolved in superdehydrated *N*,*N*-dimethylformamide (DMF) (75 mL) in a two-neck round-bottom flask under N_2. To the solution, *tert*-butyldimethylchlorosilane (4.52 g, 30.0 mmol) was added and stirred in an ice bath for 1 h, and then allowed to warm up to room temperature and stirred for 2 h. The mixture was quenched with water, extracted with hexane, washed with water, and dried over anhydrous magnesium sulfate. After the removal of the solvent under reduced pressure, the crude oil was further purified by silica gel column chromatography with hexane (R_f = 0.3), which afforded a colorless oil in 95% yield (4.75 g, 18.9 mmol): 400 MHz ^{1}H NMR ($CDCl_3$) δ = 0.02 (s, 6H, –Si–(CH_3)$_2$), 0.89 (s, 9H, –Si–C–(CH_3)$_3$), 1.30–1.60 (m, 6H, –CH_2–CH_2–CH_2–), 1.75–1.82 (m, 2H, Cl–CH_2–CH_2–), 3.54 (t, J = 6.4 Hz, 2H, Cl–CH_2–), 3.61 ppm (t, J = 6.4 Hz, 2H, –CH_2–O–).

Synthesis of 4,4′-bis(6-(*tert*-butyldimethylsiloxy)hexyloxy) benzophenone (BP-$(OTBS)_2$)

ClC_6OTBS (2.33 g, 9.29 mmol), 4,4′-dihydroxybenzophenone (0.337 g, 1.57 mmol), potassium carbonate (1.30 g, 9.41 mmol), and potassium iodide (0.081 g, 0.49 mmol) were dissolved in DMF 25 mL in a two-neck round-bottom flask, and stirred at 60 °C for 48 h. The mixture was quenched with water, extracted with hexane, washed with water, and dried over anhydrous magnesium sulfate. After the removal of the solvent under reduced pressure, the crude oil was further purified by silica gel column chromatography with hexane/ethyl acetate = 10/1 (v/v), which afforded a white solid in 75% yield (0.751 g, 1.17 mmol): 400 MHz ^{1}H NMR ($CDCl_3$) δ = 0.05 (s, 12H, –Si–(CH_3)$_2$), 0.90 (s, 18H, –Si–C–(CH_3)$_3$), 1.38–1.61 (m, 12H, –CH_2–CH_2–CH_2–), 1.79–1.86 (m, 4H, –CH_2–CH_2–O–Si–), 3.62 (t, J = 6.4 Hz, 4H, –CH_2–CH_2–O–Si–), 4.03 (t, J = 6.4 Hz, 4H, –CH_2–O–Ar–), 6.94 (d, J = 8.8 Hz, 4H, *Ar*), 7.77 ppm (d, J = 8.4 Hz, 4H, *Ar*). 100 MHz ^{13}C NMR ($CDCl_3$) δ = −5.28 (–Si–(CH_3)$_2$), 18.35 (–CH_2–CH_2–CH_2–O–Si–), 25.56, 25.80 (–Ar–O–CH_2–CH_2– and –Ar–O–CH_2–CH_2–CH_2–), 25.96 (–Si–C–(CH_3)$_3$), 29.11 (–Si–*C*–(CH_3)$_3$), 32.70 (–CH_2–CH_2–O–Si–), 63.07 (–CH_2–O–Si–), 68.10 (–Ar–O–CH_2–), 113.85 (*Ar*), 130.51 (*Ar*), 132.20 (*Ar*), 162.37 (*Ar*), 194.50 (*C*═O).

Synthesis of 1,1-bis(4-(6-(tert-butyldimethylsiloxy)hexyloxy) phenyl)ethylene (DPE-$(OTBS)_2$)

BP-$(OTBS)_2$ (3.02 g, 4.70 mmol) was heated under reduced pressure in a two-neck round-bottom flask, and then potassium *tert*-butoxide (1.07 g, 9.54 mmol) and methyltriphenylphosphonium bromide (5.04 g, 14.1 mmol) were added and the mixture was dissolved in dehydrated tetrahydrofuran (THF) 120 mL under N_2 in an ice bath and stirred at 0 °C for 1 h, and then allowed to warm up to room temperature and stirred for 16 h. The mixture was quenched with water, extracted with diethyl ether, washed with water, and dried over anhydrous magnesium sulfate. After the removal of the solvent under reduced pressure, hexane was added to the crude oil, and the precipitate was removed by filtration. After another removal of the solvent under reduced pressure, the crude oil was further purified by silica gel column chromatography with hexane/ethyl acetate = 20/1 (v/v), which afforded a colorless viscous oil in 99% yield (2.98 g, 4.65 mmol). To make DPE-$(OTBS)_2$ applicable to living anionic polymerization, it was refined by additional silica gel column chromatography with hexane/ethyl acetate = 20/1 (v/v) and subsequently heated using a heat gun under reduced pressure. Then it was degassed by the freeze–pump–thaw method and dissolved in THF, that was degassed in the presence of *sec*-butyllithium by the freeze–pump–thaw method and purified by trap-to-trap distillation, to make it

easier to put DPE-$(OTBS)_2$ in the reactor. The THF solution was kept under Ar and used in living anionic polymerization: 400 MHz ^{1}H NMR ($CDCl_3$) δ = 0.05 (s, 12H, –Si–(CH_3)$_2$), 0.90 (s, 18H, –Si–C–(CH_3)$_3$), 1.36–1.61 (m, 12H, –CH_2–CH_2–CH_2–), 1.76–1.83 (m, 4H, –CH_2–CH_2–O–Si–), 3.62 (t, J = 6.4 Hz, 4H, –CH_2–CH_2–O–Si–), 3.97 (t, J = 6.4 Hz, 4H, –CH_2–O–Ar–), 5.28 (s, 2H, C=CH_2), 6.84 (d, J = 8.8 Hz, 4H, *Ar*), 7.26 ppm (d, J = 9.2 Hz, 4H, *Ar*). 100 MHz ^{13}C NMR ($CDCl_3$) δ = −5.27 (–Si–(CH_3)$_2$), 18.35 (–CH_2–CH_2–CH_2–O–Si–), 25.59, 25.86 (–Ar–O–CH_2–CH_2– and –Ar–O–CH_2–CH_2–CH_2–), 25.96 (–Si–C–(CH_3)$_3$), 29.27 (–Si–C–(CH_3)$_3$), 32.73 (–CH_2–CH_2–O–Si–), 63.11 (–CH_2–O–Si–), 67.84 (–Ar–O–CH_2–), 111.41 (C=CH_2), 113.94 (*Ar*), 129.36 (*Ar*), 134.06 (*Ar*), 149.02 (C=CH_2), 158.79 (*Ar*).

General procedure of living anionic polymerization

All the process of living anionic polymerization except for the first step were conducted under Ar. Lithium chloride (5 eq.) was heated using a heat gun under reduced pressure in a Schlenk flask, and THF (dehydrated stabilizer free) 20 mL was added at room temperature. The solution was cooled down to −78 °C and dehydrated by sufficient *sec*-butyllithium. After inactivating *sec*-butyllithium by stirring the solution at room temperature, it was cooled down to −78 °C once more. *sec*-Butyllithium (1 eq.) was added to the solution as initiators, and then, styrene, DPE-$(OTBS)_2$ (or DPE) (5 eq.), and MMA were added to the solution successively, and stirred for 30 minutes each. At each step of polymerization, the formation of anionic species was confirmed by the colors of the solution, which are orange, deep red, and light green (or colorless), respectively. The reaction was quenched with methanol, and polymers were precipitated out in 400 mL methanol. The precipitates were dried under reduced pressure and further refined by Soxhlet extraction with cyclohexane. PS-$(OTBS)_2$-PMMA or PS-*b*-PMMA was obtained as a white solid in 76% yield.

Synthesis of PS-$(OH)_2$-PMMA

PS-$(OTBS)_2$-PMMA (202 mg, 5.05 μmol) was dissolved in THF 1.25 mL. Tetrabutylammonium fluoride in THF (0.75 mL, 150 μmol) was added to the solution and stirred at room temperature for 24 h under Ar. The product was precipitated out in methanol. The precipitate was dried under reduced pressure and PS-$(OH)_2$-PMMA was obtained as a white solid in 98% yield (197 mg).

Synthesis of P(S-*r*-MMA-*r*-HEMA)

P(S-*r*-MMA-*r*-HEMA) was synthesized *via* free radical polymerization using AIBN as initiators. AIBN (51.2 mg, 0.31 mmol), styrene (1.83 mL, 16.0 mmol), MMA (0.32 mL, 3.0 mmol), and HEMA (0.12 mL, 1.0 mmol) were added to a test tube and degassed by Ar bubbling for 5 minutes. The solution was then stirred for 8 h at 80 °C under Ar and quenched by cooling down to 10 °C. The solid product was dissolved in THF 20 mL and precipitated out in 400 mL methanol. The precipitate was dried under reduced pressure and P(S-*r*-MMA-*r*-HEMA) was obtained as a white solid in 89% yield (1.78 g).

Results and discussion

To synthesize PS-$(OH)_2$-PMMA, DPE-$(OTBS)_2$, which has two hydroxy groups protected by a TBS (*tert*-butyldimethylsilyl) group, it was synthesized in advance so that the hydroxy groups will not terminate the living anionic polymerization, according to Scheme 1. Derivatives of DPE react quantitatively with polystyryl anions, and the resulting anions are still capable of synthesizing methyl methacrylate,[28] thus the two hydroxy groups can be precisely introduced into the junction point of two blocks. DPE-$(OTBS)_2$ was designed to have two protected hydroxy groups with an alkyl linker so that the hydroxy groups would not be concealed by polymer chains and hindered from interacting with silicon substrates. Non-functionalized PS-*b*-PMMA and P(S-*r*-MMA-*r*-HEMA) were synthesized *via* living anionic polymerization or free radical polymerization, respectively. The characteristics of the synthesized polymers are shown in Table 1. The synthesized PS-$(OH)_2$-PMMA has almost the same *d*-spacing as PS-*b*-PMMA, indicating that the introduced hydroxy groups did not dramatically affect the bulk morphology.

First, polymer thin films were thermally annealed at 250 °C under N_2 for various times to form an NL on silicon substrates with a native oxide layer, and the films were rinsed by PGMEA to remove the unadsorbed polymers. PS-$(OH)_2$-PMMA thin films (~30 nm) were subsequently applied onto various NLs and annealed at 230 °C under N_2 for 10 minutes to facilitate microphase-separation in the thin films (Fig. 1).

The surface structures of the PS-$(OH)_2$-PMMA thin films supported on various NLs are observed by atomic force microscopy (AFM). PS-$(OH)_2$-PMMA thin films supported on P(S-*r*-MMA-*r*-HEMA) neutral layers that are annealed for 4 minutes or more display a fingerprint-like pattern all over the

Table 1 Characteristics of synthesized polymers for NLs

Sample	M_n[a] (kg mol^{-1})	$Đ$[a] = M_w/M_n	f_{PS}[b]	x_{OH}	*d*-Spacing[e] (nm)
PS-$(OH)_2$-PMMA	41.4	1.03	0.52	0.005[c]	22.7
PS-*b*-PMMA	40.3	1.03	0.48	0	24.4
P(S-*r*-MMA-*r*-HEMA)	28.6	2.57	0.85	0.05[d]	—

[a] Determined by SEC. [b] The volume fractions of PS in the polymers was determined by ^{1}H NMR spectra in $CDCl_3$. [c] The mole fraction of hydroxy groups in PS-$(OH)_2$-PMMA was determined by M_n and f_{PS}. [d] The mole fraction of hydroxy groups in P(S-*r*-MMA-*r*-HEMA) was determined by the preparation ratio of monomers. [e] Determined by SAXS.

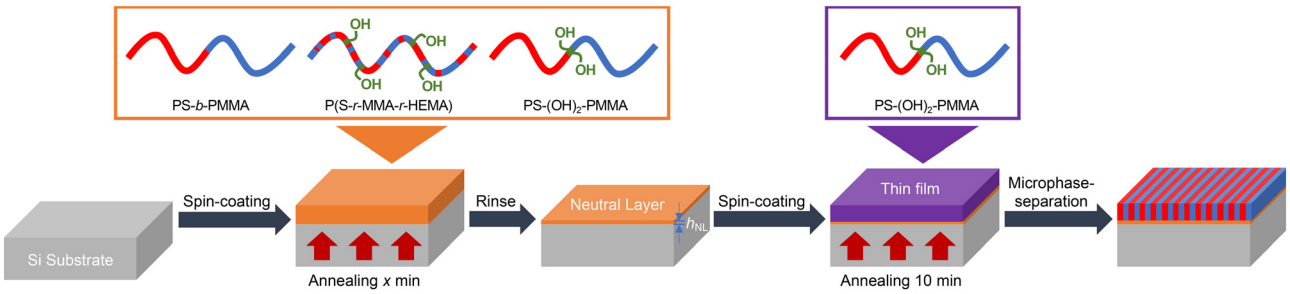

Fig. 1 Sample preparation for AFM and the materials for neutral layers (in the orange frame) and thin films (in the purple frame).

substrates, which is a typical feature of perpendicular lamellae (Fig. 2(a)). However, some holes, which are the characteristics of parallel orientation, are observed when the annealing time is shorter than 4 minutes. Still, perpendicular lamellae are observed in most part of the substrates which were annealed shortly, indicating the good adsorbability of the P(S-*r*-MMA-*r*-HEMA) neutral layer presumably arising from the hydroxy groups of HEMA units.

On the other hand, PS-$(OH)_2$-PMMA thin films supported on the identical PS-$(OH)_2$-PMMA neutral layers display a dramatic change in lamellar orientation (Fig. 2(b)). When the annealing time is 1 minute, parallel lamellae are observed all over the substrate. When the annealing time is between 2 and 15 minutes, parallel and perpendicular lamellae coexist, and furthermore, the ratio of the perpendicular region increases as the annealing time is extended. Then, when the annealing time is 20 minutes or longer, perpendicular lamellae are observed all over the substrate. This tendency of transition from parallel to perpendicular is not observed in thin films applied onto other NLs, and it seems that this tendency corresponds to the progress of the adsorption of the PS-$(OH)_2$-PMMA neutral layer. Considering the quantity of hydroxy groups introduced in each polymer for NLs, PS-$(OH)_2$-PMMA probably has intermediate adsorbability to the silicon substrates, thus the transition can be observed in this time scale. Although the perpendicular orientation under these experimental conditions is metastable (stable within one hour of annealing at 230 °C), this duration of annealing is much longer than that required for practical application of BCP lithography (within approximately 10 minutes). Therefore, it is assumed that PS-$(OH)_2$-PMMA thin films and NLs can be applicable to BCP lithography.

In contrast to these two series, the lamellae oriented parallel to the substrates in PS-$(OH)_2$-PMMA thin films supported on PS-*b*-PMMA neutral layers regardless of the annealing time of NLs in this time scale (Fig. 2(c)). These results are contrary to

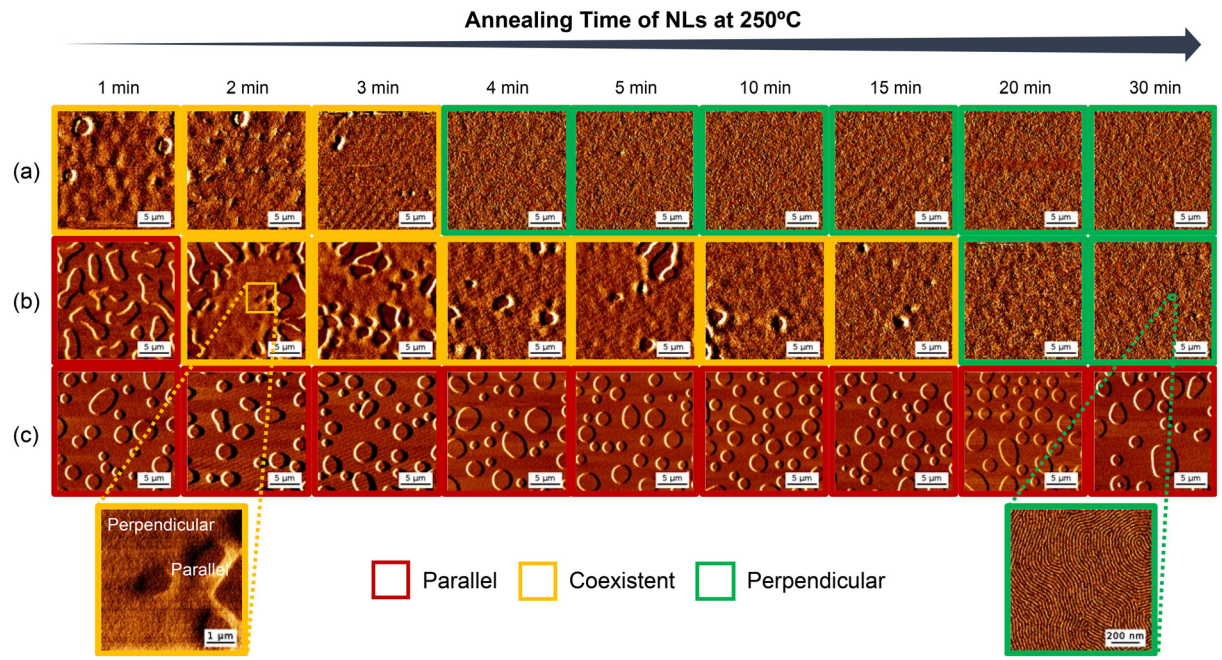

Fig. 2 AFM phase images (20 μm square) of PS-$(OH)_2$-PMMA thin films (~30 nm) applied onto (a) P(S-*r*-MMA-*r*-HEMA) neutral layers, (b) PS-$(OH)_2$-PMMA neutral layers, and (c) PS-*b*-PMMA neutral layers, which were annealed for various times from 1 to 30 minutes, accompanied by the magnified AFM phase images of coexistent orientation (5 μm square, bottom left) and perpendicular orientation (1 μm square, bottom right).

those demonstrated in the previous study,[25] which can be attributed to insufficient annealing time of NLs. It is assumed that the adsorption of NLs has not proceeded sufficiently because no hydroxy groups are introduced into PS-*b*-PMMA.

In this study, PS-$(OH)_2$-PMMA was first applied as NLs and then applied as thin films, but ideally, they can be applied at the same time by a single cast and annealing process. Perpendicular lamellae have been partially formed in a PS-$(OH)_2$-PMMA thin film (~40 nm) that was directly cast onto a Si substrate and annealed at 250 °C for 30 minutes (Fig. S20†). However, perpendicular lamellae were not completely formed across the entire area of the substrate. It is assumed that the layer that might work as an NL is not sufficiently formed in the one-step annealing due to the unsuitable annealing conditions. Nevertheless, there is a definite possibility that perpendicular lamellae can be obtained by one-step annealing, which would simplify the lithographic process.

The water contact angles (WCAs) of the NLs are plotted as a function of the annealing time of the NLs at 250 °C (Fig. 3(a)) to investigate what causes the difference in lamellar orientation. The WCAs of the NLs exhibit an almost constant value regardless of the annealing time. Those values are within the range suitable for the perpendicular orientation of lamellae in thin films of PS-*b*-PMMA system.[11,12]

However, parallel orientation is observed in PS-$(OH)_2$-PMMA thin films on PS-*b*-PMMA neutral layers or the PS-$(OH)_2$-PMMA neutral layers annealed for a short time. This contradiction can be explained as NLs are formed through the whole surface of the substrates from the early stage of the annealing, although the progression of the NL formation is insufficient to neutralize the affinities of each block component. Therefore, water contact angles cannot be an absolute indicator of the orientation of microphase-separated structures, and the difference of orientation should be evaluated from another perspective.

Next, the thicknesses of the NLs (h_{NL}) are plotted as a function of the annealing time of the NLs at 250 °C in Fig. 3(b). The h_{NL} of the NLs rapidly increases at the early stage of annealing, and then approaches a certain plateau for each NL material. The different values of the plateau indicate the distinction in the quasi-maximum amount of polymer adsorption within this time scale. P(S-*r*-MMA-*r*-HEMA) and PS-$(OH)_2$-PMMA neutral layers show larger h_{NL} than PS-*b*-PMMA neutral layers, and this difference can be attributed to whether the neutral layer contains hydroxy groups or not. However, the h_{NL} of P(S-*r*-MMA-*r*-HEMA) and PS-$(OH)_2$-PMMA neutral layers are not as different from each other as they are from that of PS-*b*-PMMA neutral layers. Therefore, it is indicated that the existence of hydroxy groups is influential in polymer adsorption to the silicon surface by thermal annealing. However, these two neutral layers induce different lamellar orientations depending on the annealing time for neutral layer adsorption, so further discussions are required to explain this discrepancy.

In addition, the surfaces of NLs formed from PS-$(OH)_2$-PMMA after the shorter (1 min, h_{NL} ~5 nm) and longer annealing (30 min, h_{NL} ~8 nm) were observed by AFM (Fig. S19†). Both NLs have a smooth surface with the surface roughness around 0.3 nm, and the surface roughness of the NLs exhibits little difference. Therefore, we suppose that the contribution of surface roughness to the perpendicular orientation of the lamellar microdomains is sufficiently minor to be disregarded in this study.

Based on these analyses of NLs, the transition of lamellar orientation observed by AFM is discussed as follows. For PS-$(OH)_2$-PMMA and PS-*b*-PMMA neutral layers, when h_{NL} is less than about 5 nm, parallel lamellae are observed. This can be attributed to insufficient NL formation, meaning there are only flattened chains in the layers and might be many molecular-sized openings where NLs are not properly adsorbed due to low or no hydroxy group content. These conditions induce an imbalance of interfacial free energy between substrates and BCP thin films, though the openings cannot be detected by WCA or h_{NL} measurement, as these measurements detect average information on the whole layer. For PS-$(OH)_2$-PMMA and P(S-*r*-MMA-*r*-HEMA) neutral layers,

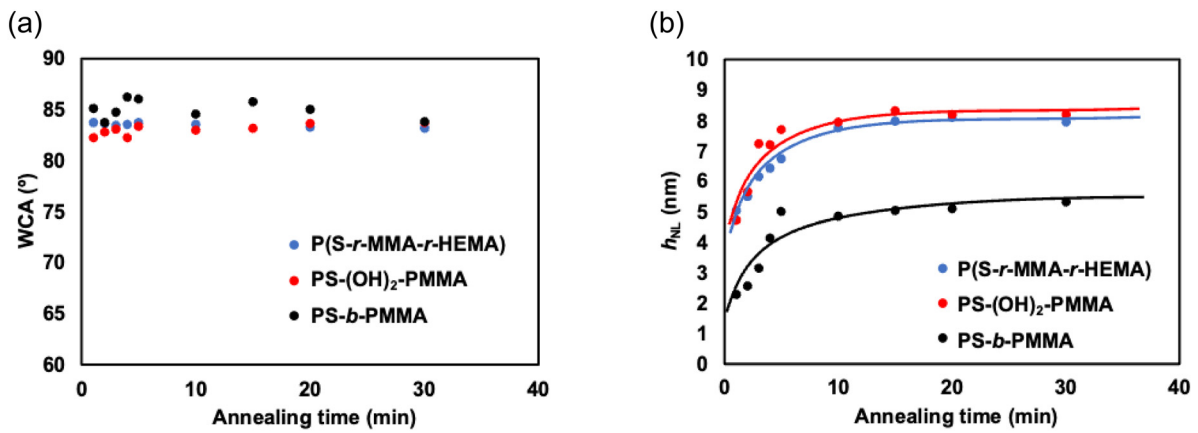

Fig. 3 (a) Water contact angles (WCAs) of the neutral layers formed by P(S-*r*-MMA-*r*-HEMA), PS-$(OH)_2$-PMMA, and PS-*b*-PMMA annealed at 250 °C for different times. (b) Thicknesses of neutral layers (h_{NL}) formed by P(S-*r*-MMA-*r*-HEMA), PS-$(OH)_2$-PMMA, and PS-*b*-PMMA annealed at 250 °C for different times.

there is only a slight difference in the increasing trends of h_{NL}, although there is an apparent difference in lamellar orientation. This can also be attributed to the difference in adsorbability of NLs caused by the hydroxy group content; that is, the more hydroxy groups the polymer has, the more easily the polymer chains adsorb to silicon substrates, preventing the formation of openings in NLs.

The difference in lamellar orientation in thin films supported on NLs annealed for a certain time can be explained by the difference in the state of polymers in NLs. It is proposed that there are a tightly adsorbed flattened layer and a loosely adsorbed layer in irreversibly adsorbed polymer thin layers.[25,29] Molecular chains move relatively easily in the loosely adsorbed layer, and it would prevent the formation of small openings and provide better randomness on the surface of the NL. This can induce perpendicular orientation due to the balanced interfacial free energy between NLs and each block component of BCPs in the thin film. On the other hand, flattened chains cannot move as they are tightly adsorbed to the silicon surface, and they cannot fill small openings in the NL. This would cause an imbalance of interfacial free energy, resulting in the parallel orientation in the thin film. Therefore, it is assumed that the perpendicular region expands in the BCP thin films supported on PS-$(OH)_2$-PMMA neutral layers as the annealing time of NL is extended and a loosely adsorbed layer is gradually formed in NLs.

Although P(S-*r*-MMA-*r*-HEMA) can still form sufficient neutral layers to induce perpendicular orientation in BCP thin films about 15 minutes faster than PS-$(OH)_2$-PMMA, it is indicated that the introduction of only two hydroxy groups can dramatically shorten the annealing time required to form NLs for obtaining perpendicular lamellae in BCP thin films, while preserving the advantage of dual role of BCPs as both NLs and thin films. Therefore, the introduction of hydroxy groups into the block copolymers can be an effective approach to making BCP neutral layers more applicable to the BCP lithography technique.

Conclusions

In summary, we propose an effective approach to shortening the annealing time for NL adsorption, sufficient for obtaining perpendicular lamellae in BCP thin films, while achieving the dual role of NLs and thin films, by precisely introducing hydroxy groups into PS-*b*-PMMA, which is one of the promising candidates for materials for BCP lithography. This method of having BCPs work as both NLs and thin films offers excellent simplicity because it hardly requires any considerations in the composition of NL materials or any additives. PS-$(OH)_2$-PMMA neutral layers annealed for more than 20 minutes can induce the perpendicular orientation of the lamellar structure in the thin films of the identical PS-$(OH)_2$-PMMA, with the minimum annealing time being intermediate between those of PS-*b*-PMMA for 24 h,[25] and P(S-*r*-MMA-*r*-HEMA) for 4 minutes. This can be attributed to the fact that PS-$(OH)_2$-PMMA has an intermediate number of hydroxy groups, which can promote the development of loosely adsorbed layers, leading to the formation of sufficient neutral layers. The necessary annealing time for sufficient NL adsorption may be further shortened by introducing more hydroxy groups at the junction point of PS and PMMA or by increasing the number of hydroxy group introduction sites. This strategy of introducing hydroxy groups into BCPs will enable the design of better neutral layers.

Data availability

The data supporting this article have been included as part of the ESI.†

Author contributions

Conceptualization, R. M. and T. H.; methodology, R. M. and S. M.; validation, R. M.; formal analysis, R. M.; investigation, R. M.; resources, T. S., T. D., K. S., K. H., Y. N. and T. H.; data curation, R. M.; writing – original draft, R. M.; writing – review and editing, R. M., S. M., T. S., T. D., K. S., K. H., Y. N. and T. H.; visualization, R. M.; supervision, S. M., K. H., Y. N. and T. H.; project administration, T. H.; funding acquisition, T. H. All authors have read and agreed on the manuscript.

Conflicts of interest

There are no conflicts to declare.

Acknowledgements

This work was supported by JSPS KAKENHI Grant Number 20H02785, 24H00052. The FE-SEM observation was conducted at the Materials Analysis Division, Open Facility Center, Tokyo Institute of Technology.

References

1 M. W. Matsen and F. S. Bates, *Macromolecules*, 1996, **29**, 1091–1098.
2 C. Sinturel, F. S. Bates and M. A. Hillmyer, *ACS Macro Lett.*, 2015, **4**, 1044–1050.
3 C. M. Bates, M. J. Maher, D. W. Janes, C. J. Ellison and C. G. Willson, *Macromolecules*, 2014, **47**, 2–12.
4 K. Koo, H. Ahn, S.-W. Kim, D. Y. Ryu and T. P. Russell, *Soft Matter*, 2013, **9**, 9059.
5 T. L. Morkved, M. Lu, A. M. Urbas, E. E. Ehrichs, H. M. Jaeger, P. Mansky and T. P. Russell, *Science*, 1996, **273**, 931–933.
6 L. Rockford, Y. Liu, P. Mansky, T. P. Russell, M. Yoon and S. G. J. Mochrie, *Phys. Rev. Lett.*, 1999, **82**, 2602–2605.
7 S. Ouk Kim, H. H. Solak, M. P. Stoykovich, N. J. Ferrier, J. J. de Pablo and P. F. Nealey, *Nature*, 2003, **424**, 411–414.
8 M. P. Stoykovich, M. Müller, S. O. Kim, H. H. Solak, E. W. Edwards, J. J. de Pablo and P. F. Nealey, *Science*, 2005, **308**, 1442–1446.
9 S.-M. Park, M. P. Stoykovich, R. Ruiz, Y. Zhang, C. T. Black and P. F. Nealey, *Adv. Mater.*, 2007, **19**, 607–611.
10 E. Han, H. Kang, C. Liu, P. F. Nealey and P. Gopalan, *Adv. Mater.*, 2010, **22**, 4325–4329.

11 D. Y. Ryu, K. Shin, E. Drockenmuller, C. J. Hawker and T. P. Russell, *Science*, 2005, **308**, 236–239.
12 P. Mansky, Y. Liu, E. Huang, T. P. Russell and C. Hawker, *Science*, 1997, **275**, 1458–1460.
13 I. In, Y.-H. La, S.-M. Park, P. F. Nealey and P. Gopalan, *Langmuir*, 2006, **22**, 7855–7860.
14 E. Han, K. O. Stuen, Y.-H. La, P. F. Nealey and P. Gopalan, *Macromolecules*, 2008, **41**, 9090–9097.
15 S. Ham, C. Shin, E. Kim, D. Y. Ryu, U. Jeong, T. P. Russell and C. J. Hawker, *Macromolecules*, 2008, **41**, 6431–6437.
16 X. Gu, I. Gunkel and T. P. Russell, *Philos. Trans. R. Soc., A*, 2013, **371**, 20120306.
17 T. Thurn-Albrecht, R. Steiner, J. DeRouchey, C. M. Stafford, E. Huang, M. Bal, M. Tuominen, C. J. Hawker and T. P. Russell, *Adv. Mater.*, 2000, **12**, 787–791.
18 C. T. Black, K. W. Guarini, K. R. Milkove, S. M. Baker, T. P. Russell and M. T. Tuominen, *Appl. Phys. Lett.*, 2001, **79**, 409–411.
19 K. Asakawa and T. Hiraoka, *Jpn. J. Appl. Phys.*, 2002, **41**, 6112–6118.
20 C.-C. Liu, P. F. Nealey, Y.-H. Ting and A. E. Wendt, *J. Vac. Sci. Technol., B: Microelectron. Nanometer Struct.–Process., Meas., Phenom.*, 2007, **25**, 1963–1968.
21 Y.-H. Ting, S.-M. Park, C.-C. Liu, X. Liu, F. J. Himpsel, P. F. Nealey and A. E. Wendt, *J. Vac. Sci. Technol., B: Microelectron. Nanometer Struct.–Process., Meas., Phenom.*, 2008, **26**, 1684–1689.
22 P. Mansky, T. P. Russell, C. J. Hawker, J. Mays, D. C. Cook and S. K. Satija, *Phys. Rev. Lett.*, 1997, **79**, 237–240.
23 S. H. Anastasiadis, T. P. Russell, S. K. Satija and C. F. Majkrzak, *J. Chem. Phys.*, 1990, **92**, 5677–5691.
24 P. A. Rincon Delgadillo, R. Gronheid, C. J. Thode, H. Wu, Y. Cao, M. Somervell, K. Nafus and P. F. Nealey, *Proc. SPIE, Alternative Lithographic Technologies IV*, 2012, vol. 8323, p. 83230D.
25 W. Lee, Y. Kim, S. Jo, S. Park, H. Ahn and D. Y. Ryu, *ACS Macro Lett.*, 2019, **8**, 519–524.
26 Y. Kim, W. Lee, S. Jo, H. Ahn, K. Kim, J. U. Kim and D. Y. Ryu, *Macromolecules*, 2020, **53**, 6213–6219.
27 S. E. Kim, D. H. Kim and S. Y. Kim, *Adv. Funct. Mater.*, 2022, **32**, 2202690.
28 A. Hirao, S. Loykulnant and T. Ishizone, *Prog. Polym. Sci.*, 2002, **27**, 1399–1471.
29 M. Sen, N. Jiang, J. Cheung, M. K. Endoh, T. Koga, D. Kawaguchi and K. Tanaka, *ACS Macro Lett.*, 2016, **5**, 504–508.